

Simultaneous observations of atmospheric structure with UAV and the MU radar

*Hiroyuki Hashiguchi¹, Takashi Mori¹, Hubert Luce², Lakshmi Kantha³, Dale Lawrence³, Tyler Mixa³, Richard Wilson⁴, Toshitaka Tsuda¹, Masanori Yabuki¹

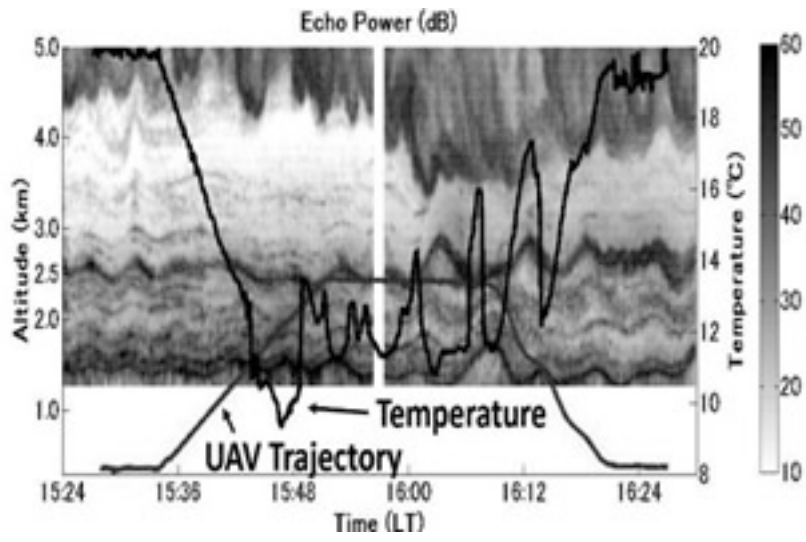
1. Research Institute for Sustainable Humanosphere, Kyoto University, 2. Université de Toulon, CNRS/INSU, IRD, Mediterranean Institute of Oceanography (MIO), 3. Department of Aerospace Engineering Sciences, University of Colorado Boulder, 4. Université Pierre et Marie Curie (Paris06); CNRS/INSU, LATMOS-IPSL

Turbulence mixing is an important process that contributes to the vertical transport of heat and substance, but it is difficult to be observed because its scale is very small. The atmospheric radar transmits the radiowave and receives backscattered echoes from turbulence to measure wind velocity profiles with high time resolution, so it has advantage in the observation of atmospheric turbulence. The MU (Middle and Upper atmosphere) radar is the atmospheric radar located at Shigaraki, Koka, Shiga Prefecture, has the center frequency of 46.5 MHz, the antenna diameter of 103 m, and the peak output power of 1 MW, and has been operated since 1984. In 2004 it is upgraded to enable radar imaging observation which provides us the improved range resolution data. The MU radar can be most accurately image the turbulence structure and is the most powerful tool to study the relationship to meso-synoptic scale phenomena. For example, although atmospheric turbulence due to the Kelvin-Helmholtz instability is known to occur in strong wind shear region, continuous turbulence structure under the cloud base has been imaged by the MU radar.

In recent years, small unmanned aerial vehicle (UAV) has been attracting attention as an observation tool of the lower atmosphere. As Japan-USA-France international collaborative research, ShUREX (Shigaraki, UAV-Radar Experiment) campaign using simultaneously small UAVs developed by the University of Colorado and the MU radar has been carried out in June of 2015 and 2016. The UAV is a small (wing width 1 m), lightweight (700 g), low cost (about \$1,000), reusable, autonomous flight possible using GPS, and it is possible to obtain a high-resolution data of the turbulence parameters by the temperature sensor of 100-Hz sampling, in addition to temperature, humidity, and barometric pressure data of 1-Hz sampling. Take-off and landing of the UAV was carried out at a pasture in 1-km southwest from the MU Observatory. The flight method previously programmed in advance takeoff before, it is also possible to change the flight method after takeoff according to the situation. It is possible to continuously fly about one hour.

The time-altitude cross-section of the echo intensity obtained with the range imaging mode of the MU radar and temporal variations of UAV altitude and temperature measured by the UAV are shown in the figure. At 15:50-16:10, the UAV was flying horizontally, but large temperature variations were observed. Temperature variations correlated with the vertical fluctuation of the strong echo layer existing around the flight altitude, and a good correlation was found with the vertical flow observed by the MU radar. From the vertical profile of the temperature measured by UAV in the following time period, it is confirmed that a deep temperature inversion layer existed and a strong echo layer accompanied it. By modeling the measured temperature profile and assuming that the temperature profile varies up and down according to the echo layer, temperature variation was reproduced. It was almost consistent with the observation result. We plan a third campaign using UAVs and the MU radar in the following fiscal year.

Keywords: MU radar, UAV, Atmospheric turbulence



Development of MU radar real-time processing system with adaptive clutter rejection

*Hiroyuki Hashiguchi¹, Kohsuke Kubota¹, Mamoru Yamamoto¹, Takahiro Manjou¹

1. Research Institute for Sustainable Humanosphere, Kyoto University

Strong clutter echoes from a hard target such as a mountain, building, or airplane sometimes cause problems of observations with atmospheric radars. In order to reject or suppress ground clutter echoes, it is effective to use NC-DCMP (Norm Constrained- Directionally Constrained Minimum Power) method, which makes null toward the direction of the clutter, if we can receive signals independently from plural antennas [Nishimura et al., JTech., 2012]. NC-DCMP method suppresses clutter echoes with maintaining the shape of main lobe to add pseudo-noise. It has been demonstrated that the NC-DCMP method is effective to real observation data with the MU (Middle and Upper atmosphere) radar, but it was processed in off-line. We successfully implemented the clutter rejection by NC-DCMP method into the on-line processing system of the MU radar. It is possible to drastically reduce the recording amount of observation data.

The MU radar is operated in a troposphere-stratosphere standard observation mode for about 100 hours every month. First we implemented the NC-DCMP processing to this standard observation mode. Observation data in this mode is obtained once every 8 seconds. Therefore it is necessary to perform all of the signal processing within 8 seconds in order to perform the clutter suppression in real-time. Now we can process the NC-DCMP in 1 second in average. Since the echoes from mountains and buildings do not change so quickly, it showed good results to determine the optimum weight vector using the received signal of the incoherent integration 7 times (about one minute). We have applied the NC-DCMP real-time processing since November 2015.

The NC-DCMP method cannot sufficiently suppress echoes from a moving target such as an airplane. In the previous study, a two-stage NC-DCMP method has been proposed as a method to suppress the airplane clutter echoes. First, airplane clutter echoes reproduced using the NC-DCMP method based on the estimated arrival direction of the airplane echo are subtracted from the original received signal. Next, ground clutter echoes are suppressed using the NC-DCMP method. In the previous study, real time processing was impossible because all directions were searched to estimate the arrival direction. Therefore, we consider limiting the search range of the arrival direction by using ADS-B (Automatic Dependent Surveillance-Broadcast) which is a system in which the airplane broadcasts the information such as position and altitude with high accuracy.

We can apply the achievement of this study to the Equatorial MU radar (EMU), which is proposed to be constructed at West Sumatera, Indonesia. The EMU system is the similar as the MU radar, but its antenna consists of 1045 Yagi antennas with 55 groups.

Keywords: Atmospheric radar, Clutter rejection, NC-DCMP method, MU radar

Statistical study on plasma bubble condition from Equatorial Atmosphere Radar, GPS scintillation, and GAIA model

*Mamoru Yamamoto¹, Dyah Rahayu Martiningrum¹, Yuichi Otsuka², Hidekatsu Jin³

1. Research Institute for Sustainable Humanosphere, Kyoto University, 2. Institute for Space-Earth Environmental Research, Nagoya University, 3. National Institute of Information and Communications Technology

We have been studying the plasma bubble over a decade by using various techniques. Equatorial Atmosphere Radar (EAR) conducted multi-beam experiment of the plasma bubble, made it possible to distinguish spatial and time variations, and clarified its near sunset-terminator occurrence of the phenomenon. EAR also found that the plasma bubbles form several-hundred km scale zonal structures, which can be considered as earlier study of large-scale wave structures (LSWS). We now conduct statistical study on the plasma-bubble condition based on observations of GPS scintillation and atmospheric condition from the GAIA model. We are finding evidences that the stratosphere around the equator show enhanced fluctuations on the day of intense plasma bubble measured by the GPS scintillations. We try to expand the comparison bases including long-term data from the EAR.

Keywords: Plasma bubble, Statistical analysis, Vertical coupling of atmosphere

New receiver system development for new satellite-ground beacon experiment

*Mamoru Yamamoto¹, Keiichi Iwata¹, Mayumi Matsunaga², Roland Tsunoda³

1. Research Institute for Sustainable Humanosphere, Kyoto University, 2. Graduate School of Science and Engineering, Ehime University, 3. SRI International

GNU Radio Beacon Receiver (GRBR) is the very successful digital receiver developed for dual-band (150/400MHz) beacon experiment. We were successfully conducted observations of total-electron content (TEC) of the ionosphere over Japan and in southeast Asia. But we now face a problem that number of beacon satellites are decreasing because of satellite aging. In order to overcome this problem we now have a project to start new satellite-ground beacon experiment with new satellite constellations. One of them is TBEx (Tandem Beacon Explorer), a project by SRI International, to fly a constellation of two 3U cubesats with triband beacon transmitters. Another one is a project of FORMOSAT-7/COSMIC-2 by Taiwan/USA. Well-known mission of COSMIC-2 is GNSS occultation experiment, but the satellites carry triband beacon transmitters. All of these satellites will be placed into low-inclination orbits by the same launch vehicle in 2018, which will give us great opportunities to enhance studies of the low-latitude ionosphere. We now develop a receiver system for experiment by using new satellites. In the presentation, we show current status of antenna and digital receiver parts of the new system.

Keywords: Satellite-ground beacon experiment, Development of instrument, Digital receiver

Automation of data analysis for satellite-ground beacon experiment

*Mamoru Yamamoto¹, Yuki Sakamoto¹

1. Research Institute for Sustainable Humanosphere, Kyoto University

We have been studying ionospheric structures by the satellite-ground beacon experiment. The main observation region is southeast Asia. For example, meridional chain of five beacon receivers along 100E meridian showed meridional distribution of total-electron content (TEC) of the ionosphere, and we revealed time and spatial variabilities of equatorial anomaly. The data analysis was, however, not easy mainly because of difficulty in estimating bias of the measurement. In this paper, we try to automate the bias estimation and lower the barrier for data analysis. The automatic bias estimation is divided in two stages. In the beginning, we make a rough estimation based on a single-station data. We assume that the TEC distributes uniform in a small section of the data, and estimated many bias candidates from all sections. The final bias is then selected based on the maximum frequent appearance basis. The second approach is the multi-station estimation. The basic idea is the same as usual two-station method, but we tried to find best match between several stations. In order to reduce computation, we start from matching between two station, and then connect the data to those from the next station. After this process, we match bias from all stations by the Brute-effort way. We now find the final bias estimation in about 80 seconds of computation by a desktop PC. Applying this multi-channel approach to the 100E meridional chain of five stations, resulted absolute TEC was close to the previous analysis obtained with much more manual efforts. We also organize these data into one NetCDF format file that helps easier use of the data.

Keywords: Satellite-ground beacon experiment, Data analysis technique, Bias estimation

Continuous monitoring of temperature profiles in the tropical troposphere with EAR-RASS

Hiraku Tabata¹, *Toshitaka Tsuda¹, Hiroyuki Hashiguchi¹, Ina Juaeni², Halim Halimurrahman²

1. Research Institute for Sustainable Humanosphere, 2. LAPAN, Indonesia

This study aims to continuously measure temperature profiles in the tropical troposphere (from 1.5 km to about 15-17 km) with high accuracy and high time-resolution by adopting Radio Acoustic Sounding System (RASS) to the Equatorial Atmosphere Radar (EAR) at KotoTabang, west Sumatra, Indonesia. We installed high-power speakers in the antenna field of EAR.

Because propagation of sound waves in the atmosphere is largely affected by the background winds, we employed the 3D ray-tracing of acoustic waves in order to predict the shape of acoustic wave fronts. Then, we selected appropriate antenna beam directions of EAR that satisfy the Bragg condition, i.e., the wave number vectors for radar waves and the target acoustic waves must be parallel.

We successfully observed the temperature profiles from 1.5 km to 5-12 km continuously with the time and height resolutions of about 3 minutes and 150 m, respectively. Temperature profiles were sometimes obtained up to about the lapse rate tropopause at 16 km. Standard deviation of the temperature difference between EAR-RASS and radiosondes was about 0.3 K. We tested the effect of sound pressure level on RASS observation. We also examined two correction methods of the background wind velocity on the sound speed.

EAR-RASS results are useful for the studies of peculiar atmospheric phenomena in the equatorial regions, such as the intense cloud convection, structure of the boundary layer, and atmospheric waves.

Keywords: RASS, EAR, tropical tropopause, temperature profile

Study of scale-sizes of ionospheric TEC gradients associated with plasma bubbles

*Susumu Saito¹, Takayuki Yoshihara¹

1. Electronic Navigation Research Institute, National Institute of Maritime, Port, and Aviation Technology

Spatial inhomogeneity or gradient of ionospheric total electron contents (TECs) is an issue in differential GNSS systems. Spatial gradients in TECs are characterized by a slope (TEC change per unit length), depth (total change in TEC), scale-size (width of the gradient), and velocity (propagation speed and direction). The slope has rather been studied well in mid- and low latitude regions. However, other parameters have not been studied well. Especially, lower bound of the scale sizes is a key factor in differentially corrected GNSS systems, because small but steep TEC gradients could fall between users and reference stations and may cause undetected user position errors.

We have installed five GNSS receivers with mutual distances of 80-1600m in Ishigaki, Japan and continue observation since 2008. We used single-frequency carrier-based and code-aided technique to derive TEC gradients. From temporal TEC variations derived from dual-frequency measurements by three receivers are used to derive velocity and scale sizes. In the case of the steepest gradient ever observed (3.38 TECU/km) associated with a plasma bubble, the velocity was estimated to be 114 m/sec in NNE direction and the scale-size was estimated to be 10 km. Analysis with more data is being conducted and the statistical results will be presented at the meeting. Possibles means to validate the results by using independent observations will also be discussed.

Keywords: Ionosphere, Plasma bubble, TEC gradient, GNSS

Preliminary results of the ionospheric observation by new ionosondes, VIPIR2, in Japan

*Michi Nishioka¹, Hisao Kato¹, Masayuki Yamamoto¹, Seiji Kawamura¹, Takuya Tsugawa¹, Mamoru Ishii¹

1. National Institute of Information and Communications Technology

National Institute of Information and Communications Technology (NICT) has been observing ionosphere by ionosondes for over 60 years in Japan. At present, four ionosondes at Wakkanai (Sarobetsu), Kokubunji, Yamagawa, Okinawa (Ogimi) are automatically operated and controlled from Tokyo. Ionospheric parameters such as foF2 and foEs are automatically scaled from the ionograms. The scaled parameters are provided through our web site (<http://wdc.nict.go.jp/IONO/>) and used for monitoring ionospheric disturbances. Currently we are replacing the current 10C type ionosondes with Vertical Incidence Pulsed Ionospheric Radar 2 (VIPIR2) ionosondes. VIPIR2 ionosonde can separate the O- and X-modes of ionospheric echoes automatically using an antenna array, which would make it easy and successful to scale the ionogram automatically. As of 2016, hardware of VIPIR2 ionosonde are installed at the four stations and its observation has started. Arrival directions of ionospheric echo were also estimated with the phase measurements of the antenna array. In the presentation, preliminary results of the VIPIR2 observation will be shown and possible collaborations will be discussed.

Keywords: ionosonde, VIPIR, HF radar

Anomalous ambipolar diffusion observed using meteor radars in northern high latitudes

*Masaki Tsutsumi¹, Yasunobu Ogawa¹, Satonori Nozawa², Chris Hall³

1. National Institute of Polar Research, 2. Institute for Space-Earth Environmental Research, Nagoya University, 3. The Arctic University of Norway

Ambipolar diffusion coefficients are estimated through radar echo decay rates of ionized meteor trails. Information of neutral atmosphere temperature in the lower thermosphere can be further deduced from the ambipolar diffusion coefficient when electron and ion temperatures can be regarded the same with the neutral atmosphere temperature [e.g., Tsutsumi et al., 1994,1996; Hocking et al., 1999, 2004]. We found that the ambipolar diffusion in the polar mesosphere was sometimes anomalously enhanced in Arctic meteor radar observations. Comparison with collocated Na lidar and EISCAT radars in Tromsø showed that such enhancements were not observed in neutral temperature field, and that enhanced electric field in the lower thermosphere seemed responsible for the anomalous ambipolar diffusion. This further indicates that meteor radar observations in polar regions have a potential to give a certain measure of electric field in the lower thermosphere and even the upper mesosphere, which is very difficult to observe without an incoherent scatter radar.

Keywords: ambipolar diffusion coefficient, meteor radars, polar mesosphere and lower thermosphere

D- and E-region ion temperature measured with EISCAT radar facility

*Yasunobu Ogawa¹, Satonori Nozawa², Masaki Tsutsumi¹, Ingemar Haggstrom³

1. National Institute of Polar Research, 2. ISEE, Nagoya University, 3. EISCAT Headquarters

The energy from the solar wind is mainly transported to the polar upper atmosphere and causes various phenomena such as auroras characterized by their rapid variability in time and space. Incoherent scatter radars (ISR) located in high latitude are one of the most powerful tools to investigate generation mechanisms of such phenomena and their effects on the atmosphere. The ISR basically gives information of plasma parameters between the bottom-side and topside ionosphere. However, ISRs have several unavoidable limitations to derive ionospheric parameters in the D- and E-region ionosphere, due to limited information in the ISR spectra. In particular, D- and E-region temperature in the polar ionosphere measured with ISRs has not been fully verified by using other temperature measurements.

We have investigated ion temperature variations in the D- and E-region using the EISCAT UHF radars located in Tromsø, Norway. Our results show that a lower limit of reliable ion temperature derivation was about 87 km altitude at noon in winter. Time variations of the daytime ion temperature at altitudes between 88 and 95 km derived from EISCAT were very close to those of ambipolar diffusion coefficients at the same altitudes from the Tromsø meteor radar data even when geomagnetic activity was high. This indicates that ion temperature at 88-95 km altitudes seems to be equal to neutral temperature at the same altitudes. We discuss what decides lower limits of the reliable ion temperature derivation, based on EISCAT data analysis under several geomagnetic/geophysical conditions.

Keywords: upper atmosphere, temperature , Incoherent scatter radar

Spectral observations of aurora and artificial aurora in EISCAT radar site, Tromsø, Norway.

*Takuo T. Tsuda¹, Shiori Hamada¹, Keisuke Hosokawa¹, Tetsuya Kawabata², Satonori Nozawa², Akira Mizuno²

1. The University of Electro-Communications, 2. Nagoya University

We have developed a compact spectrograph, which is capable of measuring optical emission intensity in visible range from ~480 nm to ~880 nm with a resolution of ~1.6 nm. The aperture, i.e. F-number, is ~4, and the data sampling rate is 1 Hz. We installed the spectrograph in European incoherent scatter (EISCAT) radar site, Tromsø, Norway (69.6N, 19.2E), and started unmanned nighttime operation on 4 October 2016. The field-of-view (FOV) of the spectrograph is pointed at magnetic field-aligned direction. Since then, aurora observations have been done continuously during this winter. In addition to the aurora observations, we plan to conduct EISCAT heater experiments for artificial aurora observations in February and March 2017. In the presentation, we will introduce spectral observations of aurora and artificial aurora in EISCAT Tromsø site.

Keywords: Spectrograph, Aurora, Artificial aurora, EISCAT

Statistical study of sporadic sodium layer (SSL) in the polar lower thermosphere and upper mesosphere by using the Tromsø sodium LIDAR

*Yohei Ogawa¹, Satonori Nozawa¹, Takuo T. Tsuda², Takuya Kawahara³, Yasunobu Ogawa⁴, Hitoshi Fujiwara⁵, Norihito Saito⁶, Satoshi Wada⁵, Toru Takahashi⁴, Masaki Tsutsumi⁴, Tetuya Kawabata¹, Chris Hall⁷, Asgeir Brekke⁷

1. Nagoya University, 2. The University of Electro-Communications, 3. Shinshu University, 4. NIPR, 5. Seikei University, 6. RIKEN, 7. The Arctic University of Norway

We will present statistical results about sporadic sodium layers (SSLs) appearing in the polar lower thermosphere/upper mesosphere during winter (November–January). The sodium LIDAR at Tromsø (69.6N, 19.2E) has made simultaneous five directional (vertical position, plus 4 horizontal positions with zenith angle = 30 deg or 12.5 deg and azimuth = 0, 90, 180, 270 deg) observations, and has obtained about 2100 hours of temperature, sodium density, and wind data between October 2012 and March 2016. Analyzing these datasets, we have identified twenty-four SSL events over the four winter seasons, and have investigated characteristics of the SSLs.

We have addressed the following questions about SSLs: (1) in-situ generation or advection, (2) ionization of aurora is needed, (3) role of Es layers and temperature, and (4) local time dependence and advent height. Concerning (1), it is important to distinguish events if they were in-situ generated or just advected into the views of the LIDAR, since so far no proposed mechanisms can explain well the rapid increase of the sodium density found in the beginning of SSL events. Based on investigation of timings of detection at each beam direction, it is found that SSLs of the 10 events seemed to be in-situ generated, while those of 14 events were advected. Concerning (2), auroras would play an important role for generation of SSLs at high latitudes, but their role is not yet well understood. At Tromsø, several instruments monitor the aurora activity. These data showed that auroras appeared in 17 events. Concerning (3), existence of sporadic E layer would be important for generation (in particular, for providing sodium atoms), but its role is not well understood quantitatively. Concerning (4), local time dependence and height of advent of SSLs are also keys to understand generation mechanisms of SSLs, in particular relationship with tide, planetary, and gravity waves. Out of the 24 events, SSLs of 9 events appeared above 100 km before 21 UT, while SSLs of the 11 events showed up below 100 km after 21 UT.

Vertical motion of the neutral atmosphere above Tromsø

*Satoru Nozawa¹, Yasunobu Ogawa², Hitoshi Fujiwara³, Takuya Kawahara⁴, Takuo T. Tsuda⁵, Norihito Saito⁶, Satoshi Wada⁶, Toru Takahashi², Masaki Tsutsumi², Tetsuya Kawabata¹, Chris Hall⁷, Asgeir Brekke⁷

1. Institute for Space-Earth Environmental Research, Nagoya University, 2. National Institute of Polar Research, 3. Faculty of Science and Technology, Seikei University, 4. Faculty of Engineering, Shinshu University, 5. The University of Electro-Communications, 6. RIKEN, 7. UiT The Arctic University of Norway

We will present results of vertical motion above Tromsø (69.6 deg. N, 19.2 deg. E) mainly based on sodium LIDAR data. Vertical motion of the neutral gases in the upper mesosphere and lower thermosphere (MLT) is a peculiar issue, and its understanding is important in terms of substance transport as well as thermal structures. Observations of the vertical wind in the MLT region are rather difficult, because vertical velocities are generally thought to be about two orders smaller than horizontal wind velocities. It is believed that the cold summer mesopause is set up by upward wind with strength of a few cm/s in the mesosphere. During high auroral activity intervals, some observations conducted by Fabry-Perot Interferometer (FPI) reported about 10 m/s or larger vertical wind velocity in the polar lower thermosphere. FPI measurements, however, suffer from a serious weakness of passive measurements: no information on the height observed. On the other hand, observations of vertical winds by radars are also difficult. Thus, our understanding of the vertical motion in the polar MLT region is still limited. The sodium LIDAR operated at Tromsø is capable of simultaneous measurements of wind velocities with five directions with a good accuracy (1-2 m/s). By using the LIDAR data (about 2100 hr data) obtained from October 2012 to March 2016 together with EISCAT, MF, and meteor radar data as well as auroral image data, we will discuss the characteristics of the vertical motion in the polar MLT.

We have found some events where the vertical wind blew with strength of about 10 m/s. In the case of January 14, 2015, the upward vertical wind with an amplitude of 10 m/s was found between 92 and 101 km over a few hours. During the night, the semidiurnal tide was strong with an amplitude of 100 m/s. This would confirm that strong vertical motion exists when such waves pass by the MLT region. In another event found in February 8, 2013, upward flows were observed between 94 and 96 km at the same time for 15 min, while no vertical flows were found at and above 97 km and at and below 93 km. Of particular interest in both cases is that a sporadic sodium layer (SSL) appeared nearby the height region where the upward vertical wind was observed at the same time (in the case of January 14, 2015) or 15 min later (in the case of February 8, 2013). In this presentation, we will address what conditions are needed for the vertical motion occurring, and also discuss possible relationship with the advent of SSLs.

Keywords: Vertical wind, Mesosphere and lower Thermosphere, LIDAR, Tromsø, EISCAT

Quasi-periodic variation in electron density, conductance and electric field during pulsating aurora

*Keisuke Hosokawa¹, Yasunobu Ogawa²

1. Department of Communication Engineering and Informatics, University of Electro-Communications, 2. National Institute of Polar Research

We report simultaneous radio and optical observations of pulsating aurora (PsA) in Tromsø (69.60N, 19.20E), Norway, using an all-sky TV camera (ATV) and the EISCAT UHF/VHF systems. During an interval within this campaign period, PsA with periods of 8-17 s was observed by the ATV in the morning local time sector (approximately 05 MLT). In this interval, quasi-periodic oscillations were identified in the raw electron density obtained by the EISCAT UHF system. The electron density at the lower part of the E region (95-115 km) was enhanced by a factor of 3-4 immediately after the optical pulsation became "on". The height-integrated Hall conductance was also elevated by a factor of 1.5-2 almost in harmony with the electron density variation. Interestingly, the remote antenna at Kiruna observed systematic redirection of the horizontal electric field when the PsA was "on". We propose a model in which the enhancement of the Hall conductance within patches of PsA caused charge accumulation at the edges of the patches, and the electric field was then modified by the resulting polarization electric field. An estimation of the electric field modulation based on this model well reproduced the actual electric field variation measured by EISCAT, which implies that the ionization caused by high-energy electron precipitation associated with PsA has a significant effect on the ionospheric current system. During the same interval of PsA, a significant ionization was observed by the EISCAT VHF system not only in the E region but also in the upper part of the D region (80-95 km). An altitude profile of the Pedersen conductance derived from EISCAT exhibited two distinct layers of enhanced conductance. The upper one occurred at ~120 km altitude which corresponded to the normal Pedersen current layer carried by the ions. The lower one appeared as a thin layer between 80 and 95 km in altitude, which was mainly carried by the collisional motion of electrons. Such an electron Pedersen layer is detectable only when the electron density is sufficiently high for allowing an appreciable current to flow in the D region. The electron Pedersen current flows exactly in the altitudes where the pulsating ionization occurs; thus, it would play more important role in the closure of electric current associated with patches of PsA.

Equatorial magnetic field variations using EE-index (MAGDAS project)

*Akiko Fujimoto¹, Akimasa Yoshikawa¹, Teiji Uozumi¹, Shuji Abe¹, Hiroki Matsushita¹

1. Kyushu University

MAGDAS project is the global ground-based magnetic field observation network and participates in the project "Study of coupling processes in solar-terrestrial system" that was approved by the Master Plan 2014 of Science Council of Japan and the Roadmap 2014 of MEXT. The MAGDAS magnetometer network allows to understand the energy transfer and propagation process from the poles to the equator, in the terms of the coupling the solar-magnetosphere-ionosphere-atmosphere.

In 2008, International Center for Space Weather Science and Education, Kyushu University (ICSWSE) proposed the EE-index (Uozumi et al., 2008; Fujimoto et al., 2016), which is an index to monitor quantitatively various equatorial geomagnetic phenomena in real time. EE-index separates the magnetic disturbances in the equatorial region into the global (EDst) and local (EUEL) magnetic variations. Especially, the detail analysis of EUEL index provides the quantitative and visible information in order to reveal the electromagnetic phenomena affecting the fundamental structure of Equatorial Electrojet (EEJ). This paper will show some examples applying EE-index to the equatorial magnetic variation: solar cycle variation of EEJ peak, semiannual EEJ variation and semidiurnal EUEL variation. The amplitude of semidiurnal EUEL variations increased in January and decreased around July. The seasonal dependence of semidiurnal variation agrees with the seasonal profile of atmospheric neutral wind (2.2) mode. The semiannual EEJ variation has two peaks in March and September. In other words, the amplitude of EEJ is weaker during solstices (January and July). We demonstrated these characteristics with time series analysis of EE-index. We are trying to understand the sources affecting the total current intensity flowing the equatorial ionosphere by separating the different contributing factors from the magnetic field variations.

Keywords: Global magnetic field observation, Equatorial electrojet (EEJ), MAGDAS project

Decomposition of the wave elements of the global high-correlation Pi 2

Teiji Uozumi¹, *Akimasa Yoshikawa¹, Shinichi Ohtani², D G Baishev³, A V Moiseyev³, B M Shevtsov⁴

1. International Center for Space Weather Science and Education, Kyushu University, 2. The Johns Hopkins University Applied Physics Laboratory, 3. Yu.G. Shafer Institute of Cosmophysical Research and Aeronomy (IKFIA), 4. Institute of Cosmophysical Research and Radio Wave Propagation (IKIR)

Global high-correlation Pi 2 pulsations are observed in wide latitudinal and longitudinal ranges on the nightside [e.g., *Uozumi et al.* 2009, 2011, 2016; *Keiling et al.*, 2014]. In those Pi 2 events, the waveforms observed at different stations were highly correlated. It is noted that localized and low-correlation Pi 2 oscillations, such as those observed near the auroral electrojet currents [e.g., *Pashin et al.*, 1982; *Samson and Rostoker*, 1983], should be treated separately from high-correlation Pi 2 events. In high-correlation Pi 2 events, systematic group delays ($|dT| \sim 100$ s) were typically observed in the H components of middle- to high-latitude Pi 2 pulsations, which typically have high correlations with low-latitude H component oscillations. While the time lags of the D component oscillations relative to the low-latitude H component oscillations were not significant ($|dT| < 10$ s) in the low- to high-latitude nighttime sector, high correlations with the low-latitude H component oscillations were observed.

The generation mechanisms of global high-correlation Pi 2 events were investigated by *Uozumi et al.* [2009, 2011]. They proposed that three possible wave elements exist in these events: (1) fast-mode waves (dB_{FW}) propagating from the Pi 2 source region in the nightside magnetosphere and observed in the low-latitude H components of Pi 2 pulsations, (2) SCW oscillations (dB_{SCW}) observed mainly in the low- to high-latitude D components of Pi 2 pulsations, and (3) directly driven Alfvénic waves (dB_{DA}) [*Kepko et al.*, 2001; *Uozumi et al.*, 2000, 2007, 2009] generated by dB_{FW} through the mode conversion process and observed as the main oscillations of the middle- and high-latitude H components of Pi2 pulsations with some group delay.

The middle- and high-latitude Pi 2 pulsations in the H component consist dB_{DA} and dB_{SCW} (dB_{DA} is dominant element in the H component Pi 2 pulsations). According to the report by *Uozumi et al.* [2016], it can be assumed that the ionospheric footprint of the upward FAC of the SCW was approximately located at the auroral onset position in each event. Thus, if we can specify the location of the auroral breakup position by using global auroral image, we can estimate dB_{SCW} in the H component from dB_{SCW} in the D component. Then one of the wave elements of dB_{DA} must be decomposed from total Pi 2 oscillations in the H component. In this study, we examined the possibility of decomposition of the wave elements of the global high-correlation Pi 2 with some typical Pi 2 events. We will present some typical cases of the decomposition. Those cases evidently demonstrate that the wave elements of the global high-correlation Pi 2 can be decomposed properly.

Keywords: global high-correlation Pi 2, aurora, substorm

Improvement of atmospheric density model in space debris evolutionary model and evaluation associated with space weather activities

*Shuji Abe¹, Toshiya Hanada², Akimasa Yoshikawa¹, Takayuki Hirai³, Satomi Kawamoto³

1. International Center for Space Weather Science and Education, Kyushu University, 2. Department of Aeronautics and Astronautics, Faculty of Engineering, Kyushu University, 3. Research Unit II, Research and Development Directorate/Japan Aerospace Exploration Agency

Space debris is the collection of defunct objects in space made by human being. It is very important to reduce amount of space debris around the Earth, because they put serious crimps in space developments. To evaluate current and future conditions of space debris on geospace and validities of space debris reduction measures, Kyushu University and JAXA developed the space debris evolutionary model, named NEODEEM (Near-Earth Orbital Debris Environment Evolutionary Model). Atmospheric drag force is one of the main cause of space debris orbit change and disappearance. Atmospheric total density changes are affected from space weather, for example, solar and geomagnetic activities. It is essential for development of space debris evolutionary model to consider the impact of space weather. Thus, we made an attempt to improve atmospheric density model to calculate more precise density and apply to our space debris evolutionary model. In the result, we developed atmospheric density model suitable for space debris orbit calculation, which includes various kinds of space weather effects not only long term variations like as solar cycle, but also short time phenomena like as geomagnetic storm. In this presentation, we will introduce improved atmospheric density model and its responses to space weather activities in term of space debris environment evaluation.

Keywords: Space Weather, Space Debris, Space Environment